

Levent Urtekin · Gokhan Kucukturk · Tuncay Karacay ·
Ibrahim Uslan · Serdar Salman

An Investigation of Thermal Properties of Zirconia Coating on Aluminum

Received: 26 November 2009 / Accepted: 9 February 2010 / Published online: 4 May 2012
© King Fahd University of Petroleum and Minerals 2012

Abstract In this study, a new coating procedure deploying plasma spraying technique for zirconia (ZrO_2) powder on aluminum substrate has been studied. Zirconia coating was applied with/without bond layer between the Ni–Al coating and the substrate. Ni–Al powders are mainly used as bond coat, which is also known as composite bonding. Thermal torch and thermal shock experiments were conducted on the coated surfaces according to ASTM C-385, and surface cracks and deformations were photographed. The experimental outcomes showed that thicker bond coating was more resistive to thermal shock and withstands longer to thermal torch. The phase change characterized by the SEM surface features was analyzed by XRD method.

Keywords Plasma spray process · Zirconia coating · Thermal barrier

الخلاصة

في هذه الدراسة تم دراسة إجراء جديد والذي ينشر تقنية رش البلازما لمسحوق (ZrO_2) على أساس الألمونيوم. تم تطبيق طلاء زيركونيا مع أو بدون طبقة الالتحام بين طلاء Ni- Al والأساس. إن مسحوق Ni- Al أساسا يستخدم كطلاء لاجم، والذي يعرف أيضا بالالتحام المركب. تم تنفيذ اختبارات على المصباح الحراري والصدمات الحرارية على الأسطح المطلية وفقا لـ ASTM C-385، وتم تصوير الشقوق السطحية والتشوهات. وقد أظهرت النتائج التجريبية بأن الطلاء الرابط الأثخن كان أكثر مقاومة للصدمات الحرارية ويقاوم أطول في المصباح الحراري. وقد تم تحليل تغيير المرحلة التي تميز ملامح الأسطح SEM وذلك بطريقة XRD.

L. Urtekin

Department of Mechanical Engineering, Faculty of Engineering, Dumlupinar University, Kutahya, Turkey
E-mail: lurtekin@du.edu.tr

G. Kucukturk (✉)

The Scientific and Technological Research Council of Turkey, Technology and Innovation Funding Directorate,
Atatürk Bulvarı No 221, 06100 Kavaklıdere, Ankara, Turkey
E-mail: gokhankucukturk@gmail.com

T. Karacay · I. Uslan

Department of Mechanical Engineering, Faculty of Engineering, Gazi University, Maltepe, Ankara, Turkey
E-mail: karacay@gazi.edu.tr

I. Uslan

E-mail: iuslan@gazi.edu.tr

S. Salman

Technical Education Faculty, Marmara University, Goztepe, Istanbul, Turkey
E-mail: ssalman@marmara.edu.tr



List of Symbols

Al	Aluminum
c	Critical fracture stress notation
E	Elasticity modulus (MPa)
h	Heat transfer coefficient (W/mK)
l	Characteristic dimension (half thickness of cover and rod diameter) (m)
k	Thermal conductivity (W/m ² K)
Ni–Al	Nickel–Aluminum
R	Thermal shock parameters
ZrO ₂	Zirconium
α	Coefficient of thermal expansion (1/°C)
β	Biot's number
ε	Thermal tension
Q	Heat transfer rate (W/m ²)
σ	Tension (MPa)
ΔT	Temperature difference (°C)

1 Introduction

Ceramic coatings on metallic materials have shown significant improvements since 1970. Some of the well-known coating techniques are physical vapor deposition (PVD), chemical vapor deposition (CVD), sol–gel (SG), plasma spray (PS), flame spray (FS), hot isostatic pressing (HIP) and detonation gun (DG). Ceramic coating helps increasing the resistance of metallic materials to wear, corrosion, oxidation and heat. In thermal barrier application coating, basic mechanical properties such as thermal expansion, thermal conductivity, corrosion resistance, wear and creep are important. Anticipated parameters of the coated material are the thermal resistance and the resistance to extreme heat. In ceramic coating using the plasma spraying technique, the conformity of metal and ceramic becomes especially important for increasing the resistance to heat and corrosion. The conformity problems usually arise from bonding difficulties of ceramics on metals due to different thermal expansion coefficients and thermal conductivities of ceramics and metals [1].

In ceramic coating, plasma spraying method provides stronger bonding when compared to flame spraying method. In literature, it is shown that Ni–Al bonding improves bonding strength of the coating [2–4]. Moreover, grain size, porosity, hardness, and fracture toughness parameters are studied and effects of these parameters to wear/friction resistance of ceramics are investigated. Grain size reduction improves mechanical properties and helps to increase wear/friction resistance [5–8].

In the 1980 s, ceramic coatings had begun to apply to adiabatic engines as thermal barriers. The size of the motor cooling system reduced due to thermal insulation, so malfunctions of the system decreased [1].

Ke et al. [9] investigated thermal shock and conductivity of thermal barriers created by coating yttria-stabilized zirconia (YSZ) over Ni-based super alloy with detonation gun spraying. Conductivity was between 1.0–1.4 W/mK, which was lower than electron beam (EB)-PVD, which is similar to plasma spraying. Moreover, this coating showed perfect thermal shock resistance. Tang and Schouenung [10] showed the thermal cycle in thermal barrier coatings and then measured Young's modulus of surface-coated YSZ material. Young's Modulus is 2,300 MPa before the thermal cycle and this is constant at 720 MPa up to 1,300 cycles.

Shanmugavelayutham et al. [11] stated that the plasma spraying condition and the parameters are very important to the final properties of coating. Zirconia, alumina, and zirconia/alumina composites were coated on stainless steel surfaces with gas tunnel type plasma spraying. The authors investigated the effects of various alumina mixture ratios to coating properties. While porosity decreased, hardness increased as the aluminum mixture ratio increased. When the porosity of the alumina coating is below 10 %, 1,400 HV hardness is obtained. Zhang et al. [12] prepared double layer thermal barrier coatings with EB-PVD at 1,323 K and different oxygen concentrations and analyzed micro structures using SEM images. Higher partial oxygen pressures sped up oxidization of the coating bond and this caused cracks between the coating and the surface.

Coating thickness is important for coating life. The thickness of the coating plays a major role in deciding the life of the coating as lower thickness does not provide complete protection and higher thickness causes reduction in the coating life due to adherence problems. So, determination of the optimum coating thickness is very important. For example, life of a super alloy is increased about 600 times with optimizing NiCoCrAl alloy coating thickness over super alloy using conduction heat corrosion experiments [13].



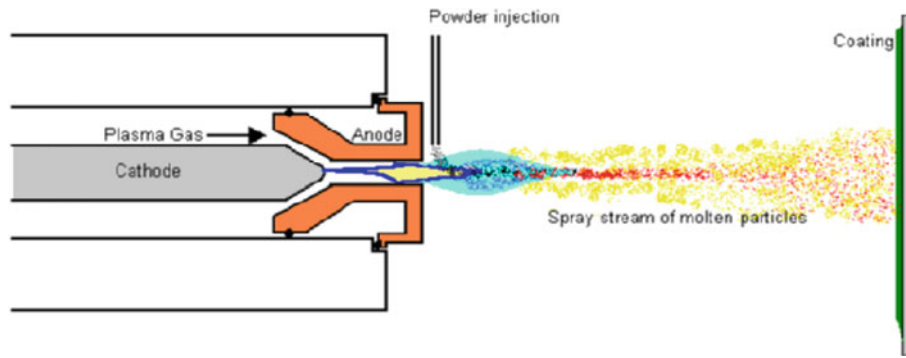


Fig. 1 Schematic view of plasma spray coating

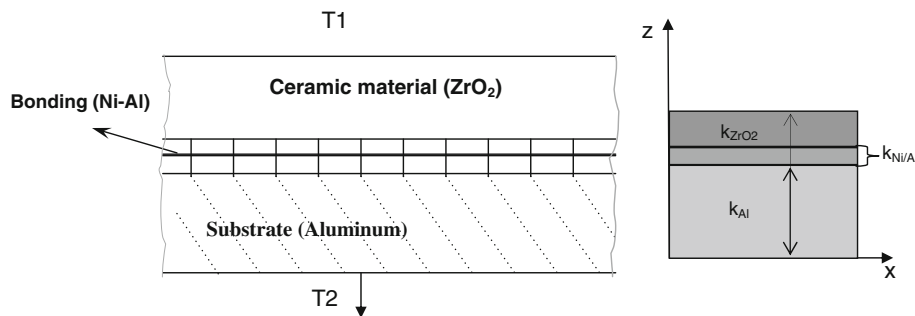


Fig. 2 Coating layer and the main layers of the surface

Zhan et al. [14] coated two different layers on super alloy surfaces with EB-PVD technique for the thermal barrier coating (TBC) purpose. Middle layer and top layer thicknesses were 60 and 120 μm , respectively. Al_2O_3 grains were sprayed to the surface to obtain different surface roughness before ceramic deposition.

In this study, aluminum substrates are coated with zirconia using plasma spraying techniques. Coating is applied with and without a bonding layer. Ni–Al powders are used as the bonding layer between the coating and the substrate. In order to observe effect of coating thickness, the specimens are coated with different zirconia coatings. Then thermal torch and thermal shock tests are applied to the specimens according to standards.

2 Plasma Spray Coating

In this technique, coating material is applied through plasma gas in powder form and sprayed on the substrate as shown in Fig. 1. In plasma spraying technique, the plasma temperature can reach over 5,500 $^\circ\text{C}$ and the impact speed of melted powder particles can reach over 240 m/s. Coating thickness is generally between 25 and 2,500 μm . Inert gases such as argon, hydrogen and nitrogen are used to form plasma spray, in order to minimize the oxidization of the coated material. However, this technique is more expensive when compared to other coating techniques. The most important advantage of this technique is that it allows working in extreme temperatures offering coating capability even for materials that melt only in high temperatures.

The surface of the substrate should be rough and free from oxides, oil and stains for good coating. Roughness is obtained by spraying high pressure air with abrasive powders such as alumina or sand.

Zirconia (ZrO_2) is obtained by melting aluminum, zirconium and silicone oxides in a furnace at 2,000 $^\circ\text{C}$. Since it contains 50 % corundum, 32 % zirconium and 18 % glass phase, it is also called melted corundum and sometimes strengthened alumina ceramic. Its wear, thermal resistance and impact strength are very good and could be used up to 1,000 $^\circ\text{C}$ easily. Heat transfer coefficient of aluminum and zirconia are 2.04 and 2.09 W/mK, respectively. The ratio between the coefficients is almost 100 [15], therefore there is a strong possibility of bonding problems with these two materials. A bond layer should be used as shown in Fig. 2 in order to prevent thermal expansion mismatch and oxidising before the application of top coating.



Heat transfer of this composite coating can be calculated using the conduction formulation as follows;

$$Q = kA \frac{\Delta T}{L} \Rightarrow Q = \frac{\Delta T}{\frac{l_{Al}}{k_{Al}A_1} + \frac{l_{NiAl}}{k_{NiAl}A_2} + \frac{l_{ZrO_2}}{k_{ZrO_2}A_3}} \quad (1)$$

And because $l_{Al} \neq l_{NiAl} \neq l_{ZrO_2}$, $\Delta T = T_1 - T_2$ and $A_1 = A_2 = A_3 = A$ the heat transferred through composite surface would be:

$$Q = \frac{\Delta T}{\frac{1}{A} \left[\frac{l_{Al}}{k_{Al}} + \frac{l_{NiAl}}{k_{NiAl}} + \frac{l_{ZrO_2}}{k_{ZrO_2}} \right]} \quad (2)$$

3 Experimental Methods and Materials

In this study, aluminum alloy substrate samples are coated with zirconia. Al_2O_3 grains are sprayed for roughening the surface before ceramic deposition. Experiments are conducted with and without bonding material between the substrate and coating. In our study, Ni–Al is selected as the bonding material. Ni–Al powder is spherical and its melting point is nearly 1,650 °C.

Plasma spray coating parameters for these experiment sets are given in Table 1. The same parameters are used for both cases.

The average size of the zirconia powder is measured with Malvern Sizer E model laser particle sizer. The average powder size is designated as d (0.5) in Table 2 and d (0.1) and d (0.9) are sizes of zirconia powders below 10 and 90 %, respectively. Powder size distribution is also obtained and given in Fig. 3.

Coating thickness is measured with the Elcometer 300 thickness measurement device. In order to investigate thermal barrier properties of zirconia coating, two different methods, thermal torch and thermal shock were used.

3.1 Thermal Torch Method

The thermal torch method is applied to measure the strength of the coating layer to hot flame. Flame is applied by means of an oxy-acetylene torch. A number 2 burner is used to provide enough punching time. Flame is applied from a distance of 10 mm. The acetylene and oxygen pressure was kept constant at 100 and 250 kPa, respectively, in order to provide a neutral flame. The oxy-acetylene torch flame is divided into three regions

Table 1 Plasma spray parameters

Coating material	Zirconia (ZrO ₂)
Material to be coated	Aluminum
Plasma type	Ar + H ₂
Argon flow rate (l/min)	50
Hydrogen flow rate (l/min)	44
Nitrogen flow rate (l/min)	–
Plasma current (A)	500
Arc voltage (V)	65
Plasma gun type	METCO 3 MB
Nozzle and electrode	W cathode–Cu anode
Nozzle diameter (mm)	8
Injector distance (mm)	100
Injector angle	90
Powder feeding ratio (g/min)	42
Powder-carrying gas (l/min)	8

Table 2 Powder size distribution and average powder size

Coating powder	d (0.5) (μm)	d (0.1) (μm)	d (0.9) (μm)
ZrO ₂	14.63	1.25	58.35



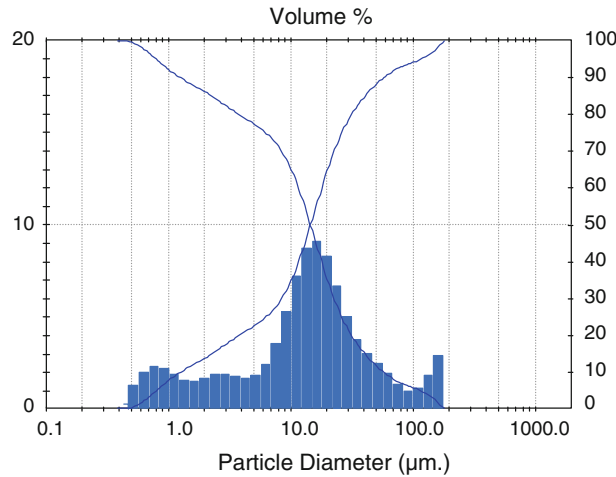


Fig. 3 Powder size distribution

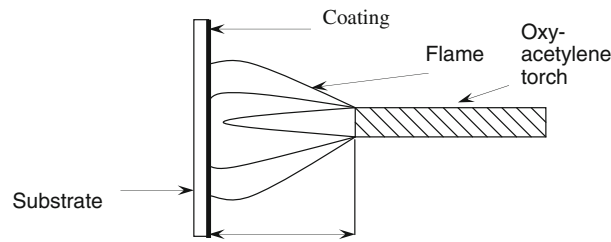


Fig. 4 Schematic view of the thermal torch experiment [16]

called spearhead, reaction and fan; and their temperatures are around 3,100–3,050 °C, 2,950–2,800 °C and 2,750 °C, respectively (Fig. 4).

The samples are prepared according to the ASTM standard [17] and their dimensions are 100×50×1.5 mm. Thermal torch experiments are applied to coated samples with/without bonding materials. Samples were not preheated prior to experiments and they were placed directly to open flame contact.

3.2 Thermal Shock Parameters and the Experiment

3.2.1 Thermal Shock Parameters

The thermal shock takes place when thermal stress reaches critical fracture stress ($\Delta T = \Delta T_c$ at $\sigma = \sigma_c$). For the simple case of a plate of material subjected to instantaneous surface temperature change, ΔT , under infinite heat transfer rate, the maximum stress is defined as:

$$\sigma = \frac{\alpha E \Delta T}{1 - \mu} \tag{3}$$

For most of the ceramic materials $\mu \cong 0.2 - 0.3$. $R_{TS} = \Delta T$ for $\sigma = \sigma_c$ accordingly, the thermal shock parameter R_{TS} ;

$$R_{TS} = \frac{\sigma_c(1 - \mu)}{\alpha E} \tag{4}$$

In practice the heat transfer rate is not infinite and the heat transfer coefficient, h (W/m²K), also controls the thermal stress development. Equation (4) is modified to include the conditions of heat transfer and conduction through the Biot's number, $\beta = \frac{hl}{k}$

$$\sigma = \frac{\alpha E \Delta T f(\beta)}{1 - \mu} \tag{5}$$

where l is the characteristic body dimension, k is the thermal conductivity, the maximum thermal stress:

$$\sigma = \frac{\alpha E \Delta T h l}{k(1 - \mu)} \quad (6)$$

Accordingly, under slow heat transfer conditions, the thermal shock parameter is defined rather as $\Delta T = R'_{TS} = k R_{TS}$, including thermal conductivity k effect on thermal shock [18–21]:

$$R_{TS} = \frac{\sigma_c(1 - \mu)k}{\alpha E} \quad (7)$$

3.2.2 Thermal Shock Experiments

Thermal barrier coatings subjected to high temperatures were exposed to thermal cycling. The thermal cycling time can be shortened for applications such as engines and turbines. A thermal shock experiment has been conducted to determine the deformation temperatures of the coatings. Thermal shock properties of the coatings were tested according to ASTM C 385 standard. The specimens were heated to the predetermined temperature and held there until temperature distribution was uniform over the specimens. Then, the specimens were immediately put into a water tank at room temperature to provide a thermal shock. The tests have been initiated at 300 °C and repeated in 20 °C incremental steps until cracks on the coating were observed.

4 Experimental Results and Discussion

The thickness and morphology of zirconia-coated surface were examined by SEM analyses which were carried out at the Chemical Engineering Laboratories of Gazi University, Ankara, Turkey. The coatings were applied with/without bonding materials in three different thicknesses, as seen in Fig. 5. It is anticipated that the thermal resistance of the samples increases in the presence of the bonding material and thick coating.

It is known that a uniform powder size and powder distribution can be achieved even though there are rough and irregular surfaces. Figure 6 shows some examples of coated surfaces. The porosity of the surface was measured according to the Archimedes principle and the porosity ratio by plasma spray is between 6 and 9 %. There is a uniform and homogeneous distribution and no deposits and no oxidation on the surface. Also no separation was found between the layers of both main material and coated material (Fig. 5). On the other hand, the sample with bonding material has a better bonding with the surface. The coated surface is suitable for thermal tests (Fig. 6).

XRD analyses were performed at the Ceramic Engineering Department of Dumlupınar University of Turkey. According to the results of the analyses, it is concluded that the coating material consists of stable zirconia and the phase has a tetragonal structure at room temperature, as seen in Fig. 7. Tetragonal structure is preferable due to its strong mechanical properties. As there will be cracked surfaces during the phase change into monoclinic structure at 1,170 °C, it is concluded that the working temperature of the coated process for

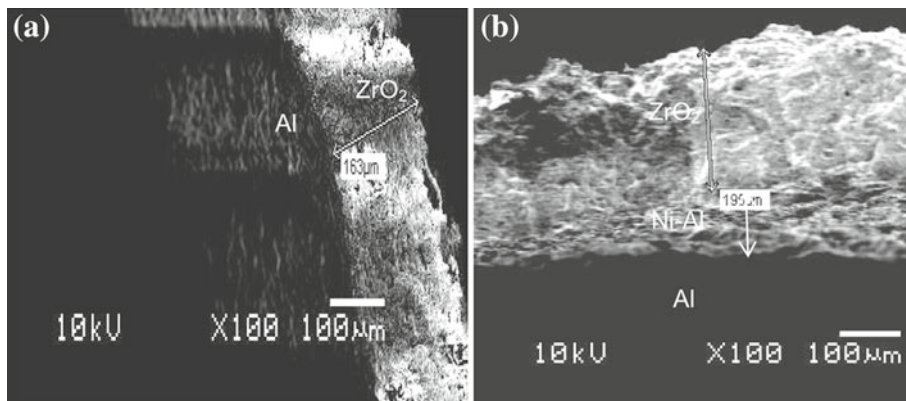


Fig. 5 Coating thickness determined by SEM analyses. **a** 163 μm —without bonding material and **b** 195 μm —with bonding material



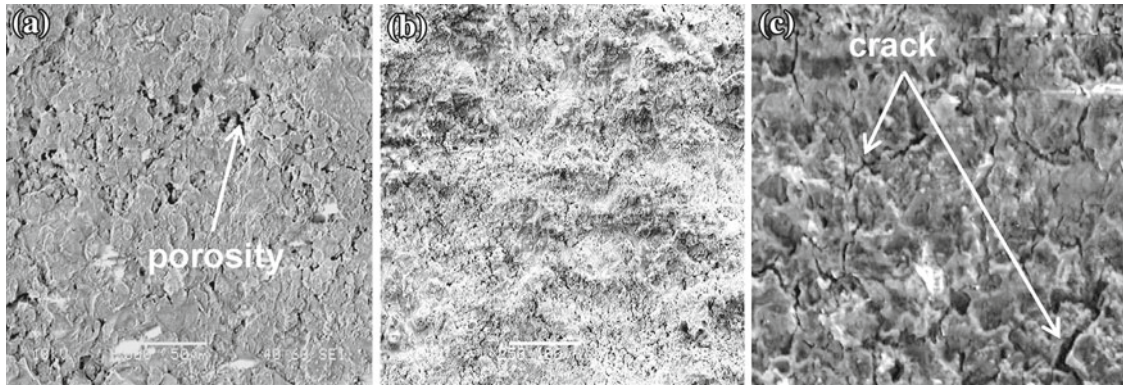


Fig. 6 SEM photos of the coated surfaces. **a** Porous structure before the experiment. **b** Surface view before the experiment. **c** Cracked surface after the experiment

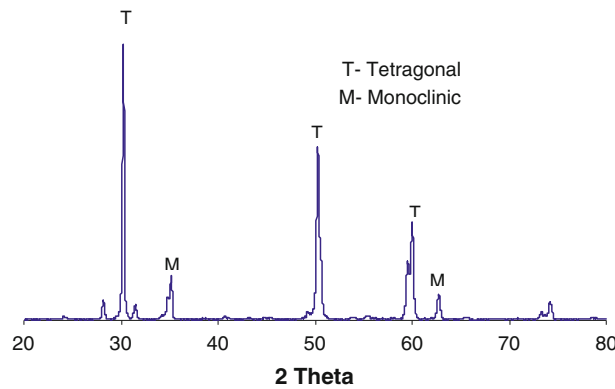


Fig. 7 XRD analyses of ZrO_2 coat

Table 3 The results of the thermal torch experiment

Coating materials	Zirconia	Zirconia-coated specimen	Zirconia	Zirconia-coated specimen	Zirconia	Zirconia-coated specimen
Coating thickness (μm)	160	160	200	200	300	300
Time required for punching a hole (s)	38	45	47	53	51	58

zirconia is 1,040 °C. In other words, the cracks forming on the surface without bonding material is not necessarily related to the structural phase change into monoclinic phase. Aluminum substrate is raised to higher temperatures than the working temperatures.

The results of the thermal torch experiments are given in Table 3 and Fig. 8. In the thermal torch experiment, three different samples corresponding to each coating thickness value are used. The mean of the deformation time values is given in Table 4. The measured thickness values belong to zirconia and the bonding material; and the total thickness values are presented both in Table 4 and Fig. 8. The evaluation of the tests is based on the time required for punching a hole through the coated specimen.

Figure 8 shows that increasing the coating thickness improves the thermal barrier coating performance of the specimen. The specimen coated with 300 μm zirconia with bonding material had the maximum performance (deformed at 58 s).

The application of the Ni–Al bonding between the substrate and the coating increases the deformation time of the thermal torch experiment. However, zirconia did not bind on the aluminum substrate in the thin coating (160 μm) without bonding layer. This is due to the low bonding strength for 200 and 300 μm coating thicknesses. An adsorption problem was not observed. Although the deformation characteristics are similar, deformation areas are always smaller in the presence of the bonding layer. There is no peeling in the coatings. However, cracks are observed around the punch after all tests. Minimum crack size is seen in the 300 μm

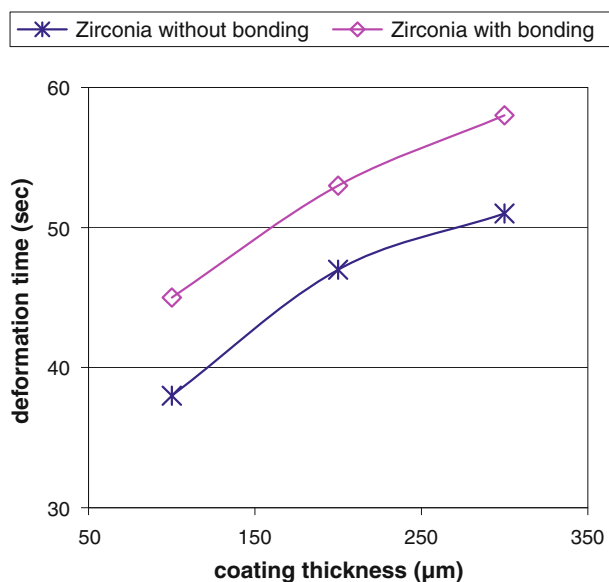


Fig. 8 The relationship between the coating thickness and the deformation time

Table 4 Thermal shock experiment results

Coating materials	Metal	With bonding material	Coating thickness (μm)	Deformation cycle	Deformation (°C) temperature
Zirconia (ZrO ₂)	Aluminum (sample a)	Ni/Al	160	34	980
	Aluminum (sample b)	Ni/Al	200	36	1,020
	Aluminum (sample c)	Ni/Al	300	37	1,040

with bonding layer. Besides, the warping that is clearly seen in the other tests was found as the lowest in this specimen compared to others.

In the thermal shock experiments, only specimens with Ni–Al bonding were used. Zirconia of three different thicknesses, 160, 200 and 300 μm, were coated over the surface of the specimens. The result of the thermal shock experiments is given in Table 4. Thermal shock cycle numbers started from 34 and continued through 37 with increasing thicknesses from 160 to 300 μm. Although bonding material (Ni–Al) is used between the substrate and coating, the anticipated bonding strength could not be obtained for the 160 μm thickness coating (Fig. 9a). Deformation is observed as peeling over the surface as well as cracks at the coating as shown in the Fig. 9. Peeling was not observed in other experiments. Cracks were smaller in the 200 μm coating when compared with the 300 μm coating. In the 300 μm thick coated specimen, thermal stress reached the critical fracture stress ($\Delta T = \Delta T_c$ at $\sigma = \sigma_c$) and cracks developed. Zirconia is known to transform from tetragonal to the monoclinic structure around 1,170 °C. During the process, volume expands and cracks develop as a result.

Aluminum has a low melting temperature at 660 °C [22], however, it is possible to use aluminum at around 1,000 °C with zirconia coating in this study. In the previous study, different ceramic coatings (Al₂O₃, CrO₂, and ZrO₂) were applied to the cast iron substrate [16] and zirconia has shown the best thermal resistance performance. In this study, aluminum with the same coating has given almost the same performance as cast iron [16]. As a lightweight material, it is very advantageous to use aluminum especially in high temperatures.

5 Conclusions

This research study focuses on the thermal barrier performance of zirconia coating on aluminum substrate. Zirconia coating is applied in various thicknesses and with/without bonding material. In order to measure the thermal barrier performance, thermal torch and thermal shock experiments were applied. The thickest coating with bonding material has given the best performance in both tests. Due to its lightweight nature, aluminum has a wide application area. Using our coating method, aluminum might resist temperatures up



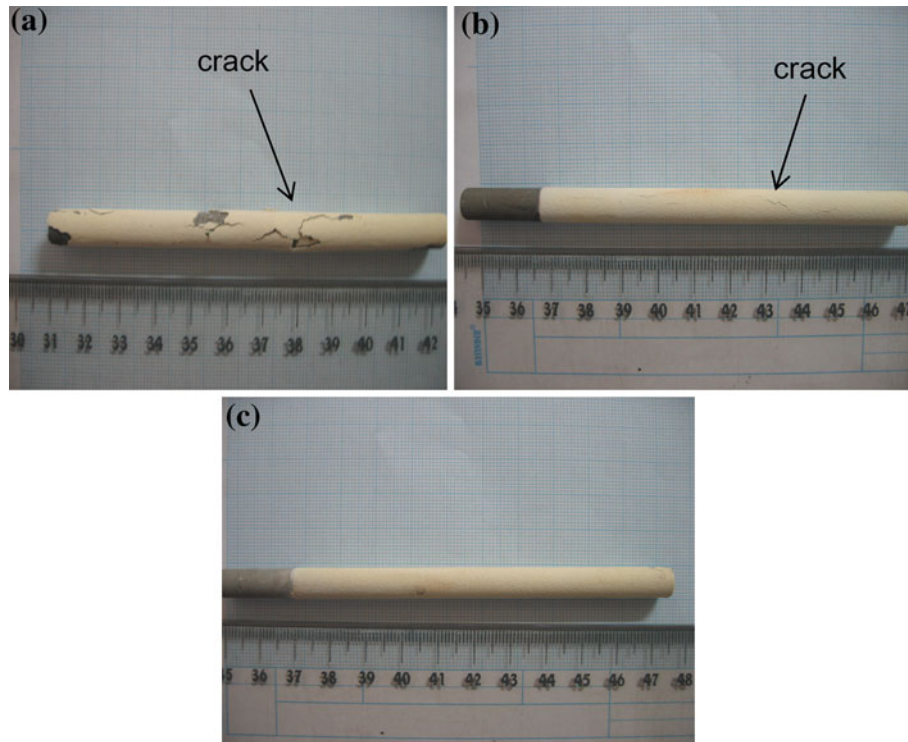


Fig. 9 Photos after the thermal shock experiment. **a** Coating thickness is 160 μm . **b** Coating thickness is 200 μm . **c** Coating thickness is 300 μm

to 1,000 °C. The phase of coated zirconia is tetragonal at room temperature, in other words it has a stable structure, as confirmed by XRD analyses. The test results show that increasing the coating thickness improves thermal resistance. Furthermore, applying a bonding layer increases the bonding strength and contributes to the thermal resistance.

In this study, the effect of powder size and shape were not taken into consideration. Size of the zirconia powder is important for the yield and the bonding strength of the coat. As for our future research plans, the effect of the powder shape in terms of porosity and bonding strength of the coating will be investigated. In this study, only Ni–Al is used as bonding material. Application of different bonding materials can increase bonding strength and thermal barrier performance of the coating. Furthermore, the application of more than one bonding material layer on aluminum substrate as a functionally graded material allows increased coating performance on aluminum substrate.

References

1. Salman, S.: The characteristics of Al_2O_3 —13wt% TiO_2 and Cr_2O_3 —5wt% SiO_2 —3wt% TiO_2 ceramic coated materials used by plasma spray technique and flame spray technique. Ph.D. Thesis Yildiz Technical University (1994)
2. Berndt, C.C.; McPherson, R.: A fracture mechanics approach to the adhesion of flame and plasma sprayed coatings. The International Conference on Manufacturing Engineering, Melbourne, Australia (1980)
3. Salman, S.; Cizmecioglu, Z.: Studies of the correlation between wear behavior and bonding strength in two types of ceramic coating. *J. Mater. Sci.* **33**, 4207–4212 (1998)
4. Gates, W.D.; Diaz-Arnold, A.M.; Aquilino, S.A.; Ryther, J.S.: Comparison of the adhesive strength of a BIS-GMA cement to tin-plated and non-tin-plated alloys. *J. Prosthet. Dent.* **69**, 12–16 (1993)
5. He, Y.; Winnubst, L.; Burggraaf, A.J.; Verweij, H.: Grain-size dependence of sliding wear in tetragonal zirconia polycrystals. *J. Am. Ceram. Soc.* **79**(12), 3090–3096 (1996)
6. Zhu, Y.; Yukimura, K.; Ding, C.; Zhang, P.: Tribological properties of nanostructured and conventional WC-Co coating deposited by plasma spraying. *Thin Solid Films* **388**, 277–282 (2001)
7. Stewart, D.A.; Shipway, P.H.; McCartney, D.G.: Abrasive wear behavior conventional and nanocomposite HVOF-sprayed WC-Co coating. *Wear* **225–229**, 789–798 (1999)
8. Dogan, H.; Findik, F.; Oztarhan, A.: Comparative study of wear mechanism of surface treated AISI 316L Stainless Steel. *Ind. Lubr. Tribol.* **55**(2–3), 76–83 (2003)



9. Ke, P.L.; Wu, Y.N.; Wang, Q.M.; Gong, J.; Sun, C.; Wen, L.S.: Study on thermal barrier coatings deposited by detonation gun spraying. *Surf. Coat. Technol.* **200**(7), 2271–2276 (2005)
10. Tang, F.; Schoenung, J.M.: Evolution of Young's modulus of air plasma sprayed yttria-stabilized zirconia in thermally cycled thermal barrier coatings. *Scripta Materialia* **54**(9), 1587–1592 (2006)
11. Shanmugavelayutham, G.; Yano, S.; Kobayashi, A.: Microstructural characterization and properties of ZrO_2/Al_2O_3 thermal barrier coatings by gas tunnel-type plasma spraying. *Vacuum* **80**(11–12), 1336–1340 (2006)
12. Zhang, C.; Zhou, C.; Gong, S.; Li, H.; Xu, H.: Evaluation of thermal barrier coating exposed to different oxygen partial pressure environments by impedance spectroscopy. *Surf. Coat. Technol.* **201**(1–2), 446–451 (2006)
13. Gurrappa, I.; Rao, S.: Thermal barrier coatings for enhanced efficiency of gas turbine engines. *Surf. Coat. Technol.* **201**(6), 3016–3029 (2006)
14. Zhang, D.; Gong, S.; Xu, H.; Wu, Z.: Effect of bond coat surface roughness on the thermal cyclic behavior of thermal barrier coatings. *Surf. Coat. Technol.* **201**(3–4), 649–653 (2006)
15. Cengel, Y.: *Heat Transfer: A Practical Approach*. McGraw-Hill Higher Education, New Delhi (2003)
16. Salman, S.; Kose, R.; Urtekin, L.; Findik, F.: An investigation of different ceramic coating thermal properties. *Mater. Des.* **27**(7), 585–590 (2006)
17. ASTM C385 Standard Test Method for Thermal Shock Resistance of Porcelain-Enameled Utensils
18. Hasselman, D.P.H.: Micromechanical thermal stresses and thermal stress resistance of porous brittle ceramics. *J. Am. Ceram. Soc.* **52**(4), 215–216 (1969)
19. Hasselman, D.P.H.: Griffith criterion and thermal shock resistance of single-phase versus multiphase brittle ceramic. *J. Am. Ceram. Soc.* **52**(5), 288–289 (1969)
20. Hasselman, D.P.H.: Griffith flaws and the effect of porosity on tensile strength of brittle ceramics. *J. Am. Ceram. Soc.* **52**(8), 457 (1969)
21. Hasselman, D.P.H.: Crack growth and creep in brittle ceramics. *J. Am. Ceram. Soc.* **52**(9), 517–518 (1969)
22. Hatch, J.E.: *Aluminium: Properties and Physical Metallurgy*, ISBN 13: 978-0-87170-176-3 (1984)

